A Continuum Approach to the Distribution of Plasma in a Pulsar Magnetosphere

Julian Faust

Department of Physics, Engineering Physics and Astronomy

Queen's University at Kingston

Under the supervision of: Dr. R. N. Henriksen

Undergraduate Research Thesis

2010 April

Abstract

The plasma density distribution in the magnetosphere surrounding a pulsar is investigated numerically using an integral of the motion due to Henriksen and Rayburn (1973). A program was written that allows calculations in which the magnetic dipole moment is neither aligned nor orthogonal to the axis of rotation, as well as the option of calculating either magnetic dipole or Deutsch field lines. The density distribution was investigated in the context of the observed eclipses of the double pulsar binary system J0737-3039 A/B when the magnetosphere of pulsar B passes through pulsar A's line of sight to Earth. The eclipse light curve yields much information on absorption in the magnetosphere of B, and this provides an impetus for a detailed study of the plasma density in B's magnetosphere. In particular, our results are contrasted with a simple model due to Lyutikov and Thompson (2005).

Contents

List of Figures **v**

1 Introduction **1**

2 PSR J0737-3039 **3**

2.1 Basic Parameters 3

2.2 Eclipse Light Curve 3

3 The Magnetosphere at Equilibrium **5**

4 Magnetic Fields **9**

4.1 Oblique Rotating Dipole 9

4.2 Deutsch Fields 9

4.3 Plasma Fields 10

5 Numerical Density Calculation **11**

5.1 Input Parameters 11

5.2 Output 12

6 Results and Discussion **13**

6.1 Dependence on ν 13

6.2 Magnetic Dipole vs. Deutsch fields 13

6.3 Comparison with McDonald and Shearer (2009) 14

6.4 Comparison with Lyutikov and Thompson (2005) 15

7 Conclusions **23**

References **25**

List of Figures

2.1 Geometry of the eclipse, with origin at pulsar B and z-axis normal to the orbital plane. The spin axis Ω_B makes an angle θ_Ω with the z-axis, and the magnetic dipole moment μ_B makes at an angle χ to Ω_B. (Figure from Lyutikov and Thompson (2005)) 3

2.2 Light intensity curves from three eclipses of J0737-0309 A by B are shown; the bottom panel is the average of the three. The dotted vertical lines represent the timing of pulses from B. (McLaughlin et al., 2004) 4

4.1 A selection of Deutsch magnetic field lines that close within the light cylinder is shown at left, where the large circle represents the light cylinder. At right, a selection of open Deutsch magnetic field lines is shown on a larger scale, where the small circle now represents the light cylinder. (figures from Henriksen and Higgins (1997)) 10

6.1 The axisymmetric case is shown for three values of ν: $\nu = 1.2$ in the left panel reaches a maximum density of 425 and a minimum density of 5×10^-7; $\nu = 1.5$ in the center frame reaches a maximum 11 and a minimum of 3×10^{-3}; $\nu = 1.8$ at right reaches a maximum of 4.54 and a minimum of 2.7×10^{-2}. 13

6.2 The axisymmetric case, with the magnetic dipole calculation at left and the calculation using Deutsch fields at right, for field lines that close within 1.5×10^7m. . 14

6.3 The orthogonal case, restricting field lines to one half of the light cylinder radius, $\sim6.7\times10^7$m. The left figures shows the dipole fields and the right figures shows the Deutsch fields; the bottom figures are the same calculations rotated by 90° so that the dipole moment is out of the page. Using $\nu = 1.8$, the dipole calculation had a relative maximum and minimum density of 250 and 1×10^{-4}, while the maximum and minimum for the Deutsch field calculation were 245 and 1×10^{-3} respectively. 15

6.4 Using Lyutikov and Thompson's best fit value $\chi = 75°$, the magnetic field lines have been allowed to extend to one half the light cylinder radius at the rotational equator. The dipole fields (left) and Deutsch fields (right) show significant differences at this radius. The bottom frames show the same calculations rotated by 90°. In the dipole calculation the relative density reached a maximum of 250 and a minimum of 1.4×10^{-4}, and in the Deutsch field calculation it reached a maximum of 252 and a minimum of 7.7×10^{-4}. 17

6.5 Using the same parameters as in 6.4, but restricting the field lines to those close within one quarter of the light cylinder radius, as measured at the rotational equator. Significant differences between the fields are still seen. The bottom frames show the same calculations rotated by 90°. In the dipole calculation the relative density reached a maximum of 36 and a minimum of 3.5×10^{-4}, and in the Deutsch field calculation it reached a maximum of 35.9 and a minimum of 7.7×10^{-4}. 18

6.6 Once again using the same parameters as in 6.4, we now restrict the field lines to those close within 1.5×10^{7}m $\sim 0.11R_{lc}$, as measured at the rotational equator. The fields appear similar at this scale. The bottom frames show the same calculations rotated by 90°. In the dipole calculation the relative density reached a maximum of 4.61 and a minimum of 9.5×10^{-4}, and in the Deutsch field calculation it reached a maximum of 4.63 and a minimum of 9.4×10^{-4}. 19

6.7 The Deutsch field lines closing within 1.5×10^{7}m are shown for $\chi = 80°$. A line is drawn representing a plane about which the density is roughly centered. A perpendicular line represents the normal to this plane, which Lyutikov and Thompson's analysis implicitly takes to coincide with the dipole moment. We find this line to be at an angle of about 68°, though placement of the line is very subjective. 20

6.8 The Deutsch field lines closing within 1.5×10^{7}m are shown for $\chi = 85°$. A line is drawn representing a plane about which the density is roughly centered, but in this case the distribution is more complicated and the uncertainty in the slope is even larger. We give a value of about 77° for angle the normal to this plane makes with the rotation axis, though we recognize that the distribution takes on a new structure as θ approaches 90°. 21

1 Introduction

A pulsar is a spinning, highly magnetic neutron star. The dipole moment is not aligned with the axis of rotation, and radiation is emitted in a beam from the magnetic poles; as a result, a distant observer sees pulses of radiation if they are within a range of angles defined by the spread of the beam. The timing of the pulses is highly regular if the pulsar is isolated in space, but measureable deviations occur if the pulsar is interacting with other bodies. For this reason, the discovery of pulsars has had far-reaching consequences in astronomy and astrophysics. In 1974 Hulse and Taylor discovered a pulsar in a highly relativistic binary system and were able to measure the variation in its pulse frequency due to the Doppler shift as the pulsar moves away and toward the Earth. The same technique has been used to identify extrasolar planets, and estimate their masses. The most extreme cases, such as the Hulse-Taylor system and the double pulsar PSR J0737-3039 A/B, can provide precise tests of General Relativity.

This thesis focuses on properties of the magnetosphere surrounding a pulsar, rather than the gravitational interaction of two pulsars or the extreme physical situation of a pulsar interior. However, in reality all three are connected and so the magnetosphere has relevance to pulsar theory in general.

The theory of pulsar magnetospheres is far from complete: the mass and charge density distributions surrounding a typical pulsar are not well known, nor does there seem to be consensus regarding the electromagnetic fields. The mechanisms of emission have been debated since their discovery, and models can be seen as more or less probable based on properties of the magnetosphere.

The plasma distribution is certainly important in understanding the emission of radiation, but the real motivation for this study is the absorption of radiation in the observed eclipses of pulsar A by B in the double pulsar PSR J0737-3039 A/B. The intensity of radiation recieved from A is modulated in time over the $\sim$30s eclipse, showing largely opaque periods as well as transparent windows at the first and second harmonics of pulsar B's spin frequency (see fig. 2.2). This gives a wealth of information about the plasma distribution in B's magnetosphere; Lyutikov and Thompson (2005) use a very simple geometrical model of the absorbing material to explain the light curve, and a primary aim of this thesis is to investigate their best fit parameters under a different set of assumptions (see sections 2.2 and 6.4).

In section 3, a model of the pulsar magnetosphere at thermal, gravitational and centrifugal equilibrium is developed following Henriksen and Rayburn (1973), resulting in a relatively simple integral of the motion which can be used to calculate the density along magnetic field lines. In

section 4, various possibilities in modelling the magnetic field are considered. Section 5 describes the computational methods used to generate data sets and plots. Finally, in section 6.4 we discuss our density distributions in the context of the eclipse light curve and the reasonably successful model due to Lyutikov and Thompson (2005).

2

PSR J0737-3039

PSR J0737-0309 is the first known double pulsar binary system, and aside from being a laboratory for precise tests of General Relativity it has provided a unique opportunity to study the absorption of radio frequency radiation from one pulsar in the magnetosphere of the other.

2.1 Basic Parameters

Pulsar B's radius is taken to be ∼10 km, and its mass is about 1.25 solar masses. It orbits with A around their center of mass with a semimajor axis of 8.8×10^8 m a eccentricity 0.088, with a period of 2.45 hours. A and B's spin periods are 23 ms and 2.8 s respectively, and both are visible in the radio spectrum[1]. B's dipole moment is estimated as approximately 3.5×10^{26} J/T.

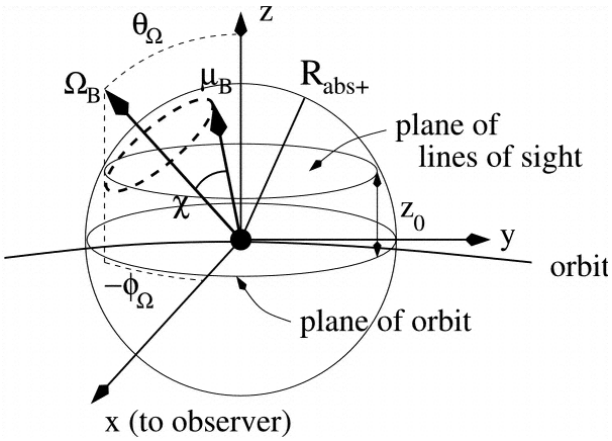

Figure 2.1: Geometry of the eclipse, with origin at pulsar B and z-axis normal to the orbital plane. The spin axis Ω_B makes an angle θ_Ω with the z-axis, and the magnetic dipole moment μ_B makes at an angle χ to Ω_B. (Figure from Lyutikov and Thompson (2005))

2.2 Eclipse Light Curve

The orbit is nearly (but not quite) edge on as viewed from Earth, so that once per orbit pulses from A pass through B's magnetosphere with some impact parameter z_0. The intensity of radiation recieved from A is modulated in time over the ∼30s eclipse, showing largely opaque periods as well as nearly transparent windows at the first and second harmonics of pulsar B's spin frequency (see fig. 2.2). These features are explained fairly well by Lyutikov and Thompson (2005) using a simple geometric model of pulsar B's magnetosphere as a rigidly rotating oblique

[1]Breton et al. (2008)

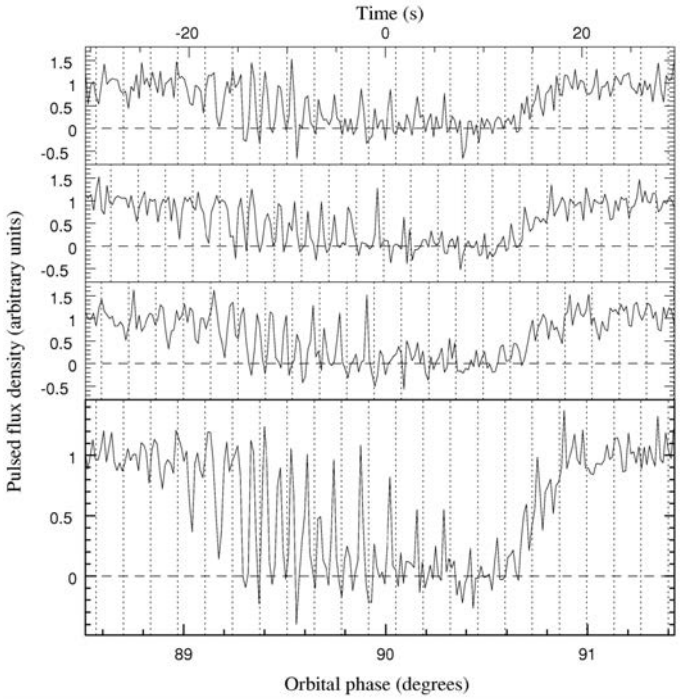

Figure 2.2: Light intensity curves from three eclipses of J0737-0309 A by B are shown; the bottom panel is the average of the three. The dotted vertical lines represent the timing of pulses from B. (McLaughlin et al., 2004)

magnetic dipole, with constant plasma density along those field lines with maximum extension between some inner and outer radius $R_- < R_{max} < R_+$, measured at the magnetic equator. Field lines closing inside or outside this radius are given zero density. These assumptions are contrary to those of this thesis, as our method gives varying density along field lines. Their model is successful enough, however, that a detailed study was carried out using our method with their best fit parameters wherever possible. The implications of our method in the context of Lyutikov and Thompson (2005) are discussed in section 6.4. They provide best fit values for the parameters R_-, R_+, the angles θ_Ω, ϕ_Ω and χ, and the impact parameter z_0 (see Fig. 2.1). Of primary interest to this thesis are R_+ and χ, since the computation described in section 5 calculates a density profile but does not go as far as to simulate the eclipse. R_+ can be used to limit the computation to a region comparable to the size of the magnetosphere (i.e. the half-width of the eclipsing material, which is determined from the duration of the eclipse and the orbital radius and period to be $\sim 1.5 \times 10^7$ m). One needs such a limit, as the assumption of corotation breaks down at the light cylinder. Additionally, under the strict assumption of corotation the density calculation diverges for field lines approaching the light cylinder, and the maximum density attained in a calculation depends strongly on the limit R_+. Lyutikov and Thompson's best fit value for the angle χ between the dipole moment and the rotation axis is $\sim 75°$, and this is taken as a starting point for our investigations.

3

The Magnetosphere at Equilibrium

The computational tool making this study of the magnetosphere possible is an integral of the motion due to Henriksen and Rayburn (1973); some key points of the derivation are summarized here. The notation primarily follows that of Fock (1964), taking the $(+ - - -)$ convention for the Minkowski metric.

We consider the region surrounding a pulsar isolated from external gravitational influences (in the context of PSR J0737-3039, we neglect the effect of pulsar A's gravity on B's magnetosphere). The surrounding matter is treated as a single fluid plasma with stress-energy-momentum tensor (see Fock (1964))

$$T_M^{\mu\nu} = (\mu^* + p/c^2)u^\mu u^\nu - pg^{\mu\nu}. \tag{3.1}$$

where p is the pressure, μ^* is the total mass density in the local inertial frame (including the mass equivalent of the plasma's compressional potential energy), and $u\mu$ is the four velocity.

The metric $g_{\mu\nu}$ is taken to be the Schwarzschild metric, with line element

$$ds^2 = g_{\mu\nu}dx^\mu dx^\nu = \left(1 - \frac{2GM}{rc^2}\right)c^2dt^2 - \frac{1}{1-\frac{2GM}{rc^2}}dr^2 - r^2(d\theta^2 + \sin^2\theta d\phi^2). \tag{3.2}$$

Defining

$$\psi \equiv 1 - \frac{2GM}{rc^2}, \tag{3.3}$$

the four velocity is

$$\begin{aligned} u^\mu &= \left(\frac{\gamma}{\sqrt{\psi}}\right)\frac{dx^\mu}{dt} \\ \gamma &= \frac{1}{\sqrt{1 - \frac{\dot{r}^2/\psi + r^2\dot{\theta}^2 + r^2\sin^2\theta\dot{\phi}^2}{c^2\psi}}}. \end{aligned} \tag{3.4}$$

Under the assumption that the plasma corotates with the pulsar, γ simplifies to

$$\gamma = \frac{1}{\sqrt{1 - \frac{r^2\sin^2\theta\Omega^2}{c^2\psi}}}. \tag{3.5}$$

This implies a light cylinder radius of $R_{lc} = \psi\frac{c}{\Omega}$, which is close to the value $\frac{c}{\Omega}$ seen throughout the literature since $\psi \approx (1 - 3\times10^{-5})$ at this radius.

3. THE MAGNETOSPHERE AT EQUILIBRIUM

The use of the Schwarzschild metric in describing the geometry around a pulsar is justified under several assumptions:

- It is a vacuum solution, so is a good approximation only if the total gravitational effect of the magnetosphere is negligible compared to that of the pulsar. We believe this to be the case, since the plasma is many orders of magnitude less dense than a neutron star interior.

- It assumes a spherically symmetric mass distribution as the source of gravitation. In reality the mass distribution is distorted due to centrifugal effects.

- It neglects the effects of the pulsar's rotation on the geometry, so we require that the pulsar's angular momentum J is not too large. A more complex treatment could be done using the Kerr metric, which reduces to the Schwarzschild metric in the limit that $\frac{J}{Mc^2r} \ll 1$. The angular momentum of a pulsar is difficult to predict since the equation of state is unknown, and thus the moment of inertia cannot be calculated. As a rough estimate, we idealize pulsar B as a uniform sphere (radius ∼10 km) with moment of inertia $I = \frac{2}{5}M_B R_B^2$ to find

$$\frac{J}{Mc^2r} \approx \frac{2}{5}\frac{R_B^2\Omega_B}{c} \approx 3 \times 10^{-5}\frac{R_B}{r} \tag{3.6}$$

  which in our calculation, is at most $3{\times}10^{-6}$. In light of this, the gravitational effects of pulsar B's rotation should be negligible; however, it should be noted that the moment of inertia is unknown by a large factor, and the Kerr geometry will begin to become significant for faster-spinning pulsars.[1]

Under these assumptions, we proceed in using the Schwarzschild metric in the corotating frame with the understanding that the calculation is restricted to the region $R_{pulsar} < r < R_{lc}$. R_{lc} is the "light cylinder" beyond which the assumption of corotation would imply velocities greater than c. Due to the strong magnetic field, we suppose that charged particles are confined to magnetic field lines, executing helical motion. Field lines that close a reasonable distance within the light cylinder may then be capable of supporting an equilibrium density of plasma.

Adding the electromagnetic field tensor to the equation 3.1 gives the total mass-energy-momentum tensor $T^{\mu\nu}$. The equations of motion follow from the conservation laws given by setting the covariant derivative of $T^{\mu\nu}$ equal to zero.

$$\begin{aligned} T^{\mu\nu} &= T_M^{\mu\nu} + T_E^{\mu\nu} \\ T^{\mu\nu}{}_{;\mu} &= 0 \end{aligned} \tag{3.7}$$

[1]The double pulsar system may allow a unique opportunity to measure the moment of inertia of pulsar A (which is faster spinning than B by a factor of over a hundred), from the relativistic effects of spin-orbit coupling; the implications of this on constraining the neutron star equation of state are described by Morrison et al. (2004). This effect will not be measureable for pulsar B.

The quantity μ^* includes the compressional potential energy of the plasma (divided by c^2), and so is not constant over the course of the motion. This difficulty is solved by Fock (1964) by introducing the invariant rest frame density ρ via

$$\frac{d\rho}{\rho} = \frac{d\mu^*}{\mu^* + p/c^2}. \tag{3.8}$$

Introducing the total internal energy per unit invariant rest mass $\epsilon = p/(\rho c^2) + \mu/\rho$, Henriksen and Rayburn (1973) write the equations of motion 3.7 explicitly and take the scalar product of the spacelike components with the local magnetic field unit vector. In the case that the average charge separation of the plasma is constant, the result can be integrated along the magnetic field line to obtain (assuming the electrostatic contribution is small)

$$\epsilon\sqrt{\psi}/\gamma \quad = \quad \text{constant on a magnetic field line,}$$

$$\epsilon \quad \propto \quad \frac{1}{\sqrt{\psi}} \frac{1}{\sqrt{1 - \left(\frac{r\Omega \sin\theta}{c\sqrt{\psi}}\right)^2}} \tag{3.9}$$

Assuming that the equation of state of the plasma takes the form $p \propto \rho^\nu$ for some $\nu \neq 1$, one can express the invariant rest frame density ρ relative to a reference point s as

$$\frac{\rho}{\rho_s} = \left(\frac{\epsilon - 1}{\epsilon_s - 1}\right)^{\frac{1}{\nu - 1}}. \tag{3.10}$$

Equation 3.10 is used for the colour scaling on all plots in this report. Under this analysis, ρ represents the density when the magnetosphere is at equilibrium with respect to thermal, gravitational, and centrifugal effects. Qualitatively, we see that the density is large when ψ is small (i.e. close to the star), as well as when γ is large (i.e. radii approaching the light cylinder). We note that the Schwarzschild radius for pulsar B is $\frac{2GM_B}{c^2} \approx 3.7\text{km} \approx 0.37R_B$, and so we expect ψ to range from 0.63 at the stellar surface to about $(1 - 3 \times 10^{-5})$ at the light cylinder. γ is equal to 1 along the rotation axis (equation 3.5 with $\theta = 0$), $\gamma \approx (1 + 4.4 \times 10^{-9})$ at the equator of the stellar surface ($\theta = \pi/2$) and $\gamma \to \infty$ as r approaches the light cylinder.

While this integral of the motion is useful in determining the density along a field line relative to a reference point, in order to build a complete picture of the density distribution in the magnetosphere one requires an assumption about the density at many reference points.

4

Magnetic Fields

Given the form of the magnetic field, equation 3.10 can be used to calculate the relative density along a field line. The choice of a suitable magnetic field in modelling the pulsar exterior has drastic consequences on any conclusions made regarding the density distribution. In the context of the calculations of this thesis, the shape of the fieldlines closing within the light cylinder determines where particles can accumulate. Under the assumption that the plasma corotates, it only makes sense to calculate within the light cylinder defined by $r \sin\theta \leq R_{lc}$. Magnetic fieldlines that close outside the light cylinder are less relevant as they cannot support a population of particles at equilibrium. The question of which fieldlines close within the light cylinder is tractable analytically only in the simplest cases, i.e. the axisymmetric case of a magnetic dipole aligned with the rotation axis.

4.1 Oblique Rotating Dipole

The simplest realistic model of the magnetic fields around a pulsar is a dipole inclined at an angle χ to the axis of rotation and rotating rigidly with the pulsar. This seems to be a fairly reasonable approximation at distances that are small compared to the light cylinder radius, but large compared to the radius of the star; Lyutikov and Thompson (2005) use a simple dipole in their model, and successfully predict many features of the eclipse light curve of PSR J0737-3039. This indicates that in the region of interest the actual field is at least approximately dipolar and rigidly rotating.

4.2 Deutsch Fields

A solution for the electromagnetic fields in all space due to an idealized magnetic star was provided by Deutsch (1955). The star is idealized as a perfectly conducting, highly magnetized rotating sphere in vacuum; that is, conductivity is infinite for $r < R_*$ and zero for $r > R_*$. In the limit that the radius of the star is much less than the radius of the light cylinder R_{lc} (for pulsar B, $R_B/R_{lc} \approx 7.5 \times 10^{-5}$), the components of the magnetic field outside the star are

$$
\begin{aligned}
B_r &= \frac{2\mu}{r^3}\left[\cos\alpha\cos\theta + \frac{r}{R_{lc}}\sin\alpha\sin\theta\sin\lambda + \sin\alpha\sin\theta\cos\lambda\right] \\
B_\theta &= \frac{\mu}{r^3}\left[\cos\alpha\sin\theta + \left(\frac{r^2}{R_{lc}^2} - 1\right)\sin\alpha\cos\theta\cos\lambda - \frac{r}{R_{lc}}\sin\alpha\cos\theta\sin\lambda\right] \\
B_\phi &= -\frac{\mu}{r^3}\left[\left(\frac{r^2}{R_{lc}^2} - 1\right)\sin\alpha\sin\lambda + \frac{r}{R_{lc}}\sin\alpha\cos\lambda\right]
\end{aligned}
$$

(4.1)

Here the polar angle θ refers to the axis of rotation, α is the angle between the rotation axis and the effective magnetic dipole moment, and $\lambda = \phi \pm \frac{r}{R_{lc}}\Omega t$ (See Higgins (1996)).

The magnetic Deutsch field reduces to a magnetic dipole for $R_{pulsar} \ll r \ll R_{lc}$. Considering that the eclipsing material of pulsar B has a half-width of $\sim 1.4\times10^7$ m [1] and the light cylinder is about 1.3×10^8 m, the Deutsch field will begin to give distinct results in the outer magnetosphere.

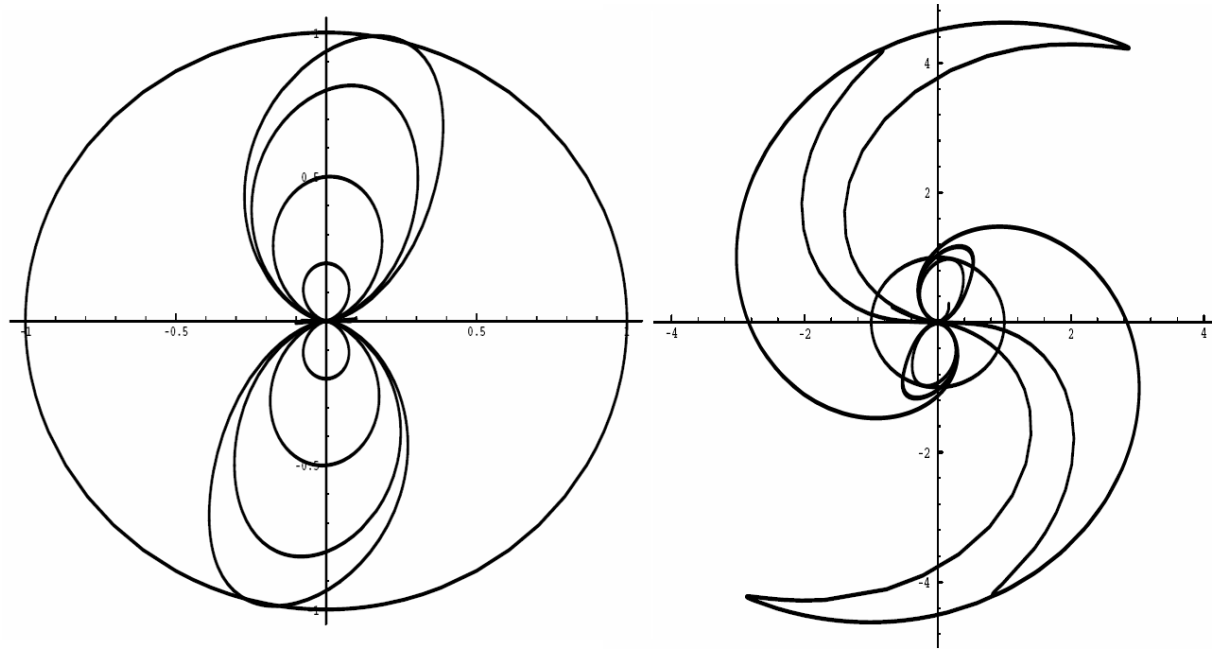

Figure 4.1: A selection of Deutsch magnetic field lines that close within the light cylinder is shown at left, where the large circle represents the light cylinder. At right, a selection of open Deutsch magnetic field lines is shown on a larger scale, where the small circle now represents the light cylinder. (figures from Henriksen and Higgins (1997))

Deutsch fields have been used in describing the exterior of a pulsar, for example by Henriksen and Higgins (1997), Quadir et al. (1980) and McDonald and Shearer (2009).

4.3 Plasma Fields

The Deutsch fields are vacuum solutions to Maxwell's Equations, and thus completely neglect the electromagnetic fields due to the flow of plasma in the magnetosphere. The plasma fields could in principle be added to the Deutsch fields by the principle of superposition; the problem is then to self-consistently solve for the charge and current densities and electromagnetic fields. This is a daunting task both analytically and computationally, and is beyond the scope of this paper. See McDonald and Shearer (2009) for a 3D computation that self-consistently finds equilibrium charge distributions using a superposition of Deutsch fields and plasma fields.

[1] Lyutikov and Thompson (2005)

5

Numerical Density Calculation

A major analytical difficulty is the loss of symmetry when the angle χ between the dipole moment and the axis of rotation is nonzero, which seems to be necessary in describing a real pulsar. For this reason the approach of this thesis is largely numerical, so that the the implications of equations 3.9 and 3.10 in the case of off-axis magnetic dipoles, as well as the more complicated Deutsch fields (see section 4.1), can be understood. A program was written in C++ making extensive use of the ROOT data analysis framework (root.cern.ch) to calculate the relative density along field lines in three dimensions.

5.1 Input Parameters

The program has as basic parameters the mass, dipole moment and rotational velocity of the pulsar, which are fixed as the best estimates for the parameters of pulsar B in section 2.1. Other parameters include:

- A set of reference points, along with the density at each point. The calculation follows the magnetic field lines starting from these points, using equations 3.9 and 3.10 to find ρ at many points in space.

- An initial step length for moving along field lines. In order to make calculations viable over a large range but still provide enough data points, the effective step length scales as $\sqrt{r}$.

- The exponent ν in our assumption that $p \propto \rho^{\nu}$. Since ρ is a monotonic function of ϵ, changing ν does not change the locations of the maxima and minima. Rather, it affects how extreme the density gradients are. See Figure 6.1

- The angle χ between the dipole moment and the rotation axis, as well as the magnitude of the dipole moment and the rotation angular velocity Ω

- A condition to only output field lines that close within a certain radius, which should be chosen to be some fraction of the light cylinder radius. One can also output the field lines not satisfying this condition if desired.

- The choice between using the magnetic dipole or Deutsch fields in the magnetic field calculation

The reference points should be chosen with the limiting radius in mind, since the field lines we are interested in are those that close near the limiting radius. Although the program checks each field line against the limiting condition before outputting it, much computational time can be saved with some knowledge of where to place the initial points to generate the field lines of interest. The limiting field lines, both in the case of a magnetic dipole and the Deutsch fields, are found to be those that are started at points reasonably close to the magnetic axis. Points started at a large angle to the magnetic axis do not extend far beyond the initial radius; Lyutikov and Thompson (2005) suggest that in this region, the magnetic field is so strong that charged particles quickly lose their energy to synchrotron radiation, and are no longer good absorbers. The field lines of interest, then, are generated by starting points at angles within a narrow range with respect to the magnetic axis. We choose all initial points at constant radius $r = 100$ km and distribute points symmetrically about the magnetic axis, i.e. for each angle in this range, the azimuthal angle (with respect to the magnetic axis) is varied at increments from 0 to 2π. This symmetrical placement of inital points is necessary in order to see the symmetries in the resulting field lines and density distribution.

The greatest difficulty here is in assigning a density to the initial points, or even their density relative to each other. The initial points are relatively close together in space, but may be in a region where the density changes rapidly. A related issue is that the integral of the motion 3.9 holds along a single field line, and it is likely that the constant of integration varies between different field lines. Varying this constant between fieldlines seems to have a similar effect to varying the initial densities; for simplicity, the initial points have been given equal density in all plots shown and the constant of integration is fixed at 1.

5.2 Output

The program outputs the x, y and z components and the relative density ρ/ρ_s of each step along every field line that satisfied the limiting condition, i.e. closed within a maximum radius $R_{max} < R_{lc}$. Due to the huge amount of data in a detailed calculation, a second program was written utilizing the 3D plotting facilities in ROOT. The density is plotted on a colour scale, with blue representing the minimum density in the calculation, green intermediary and red representing the maximum density in the calculation. Since we lack an absolute scale due to issues mentioned above, the intended interpretation is that the colours are not directly comparable between two different calculations, or even between two field lines within one computation. However, we make note of the maximum and minimum density relative to the initial points (i.e. the values corresponding to red and blue) for each calculation, and state these values relative to the initial points having relative density 1.

In all plots shown, lengths are in meters $\times 10^6$.

6

Results and Discussion

6.1 Dependence on ν

Without knowledge of the equation of state of the plasma, we must choose a value of ν in the relation $p \propto \rho^{\nu}$. Three choices of ν between 1 and 2, and the corresponding density distributions are shown in Figure 6.1.

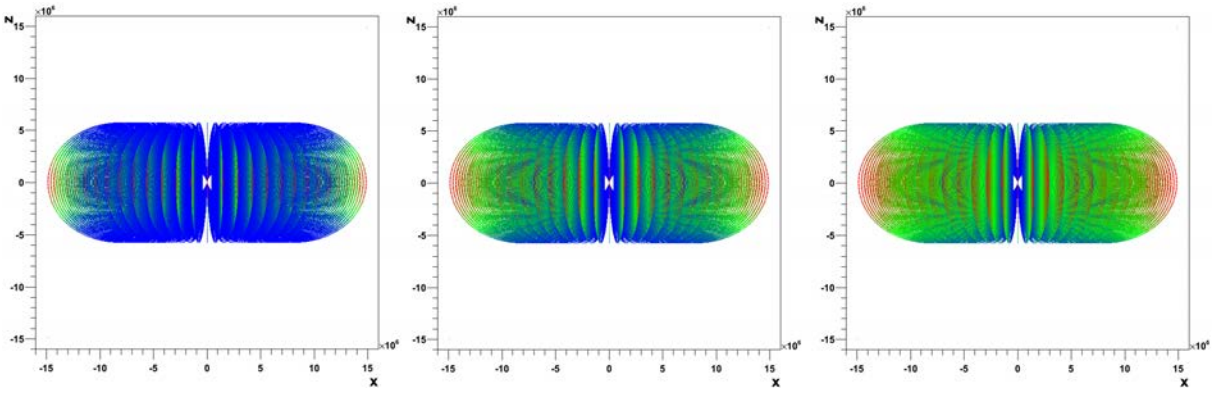

Figure 6.1: The axisymmetric case is shown for three values of ν: $\nu = 1.2$ in the left panel reaches a maximum density of 425 and a minimum density of $5{\times}10^{-}7$; $\nu = 1.5$ in the center frame reaches a maximum 11 and a minimum of $3{\times}10^{-3}$; $\nu = 1.8$ at right reaches a maximum of 4.54 and a minimum of $2.7{\times}10^{-2}$.

It is evident from equation 3.10 that ν affects the gradient of ρ, but not the locations of maxima and minima. This is seen in Figure 6.1 in the axisymmetric case, and is true in cases with no symmetry as well. The value of ν is fixed at 1.8 all of the following plots.

6.2 Magnetic Dipole vs. Deutsch fields

A major aim of this study was to determine under what conditions the Deutsch fields yield results distinct from the dipole approximation.

Figure 6.2 compares the dipole field (left) to the Deutsch field (right) in the axisymmetric case, for field lines that close within $1.5{\times}10^{7}$m $\approx 0.11 R_{lc}$. At this radius the fields are virtually identical. In the axisymmetric case, it is difficult to see how the Deutsch fields could differ greatly from a dipole unless the limiting radius R_{+} is increased almost to the light cylinder, since the maximum extension of the fieldlines is perpendicular to the axis of rotation. However, if the angle χ is increased then the magnetosphere is allowed to extend along the axis of rotation, and field lines could reach a radius beyond the regime $r \ll R_{lc}$ while still ensuring $r \sin\theta$ is less than some reasonable fraction of the light cylinder radius.

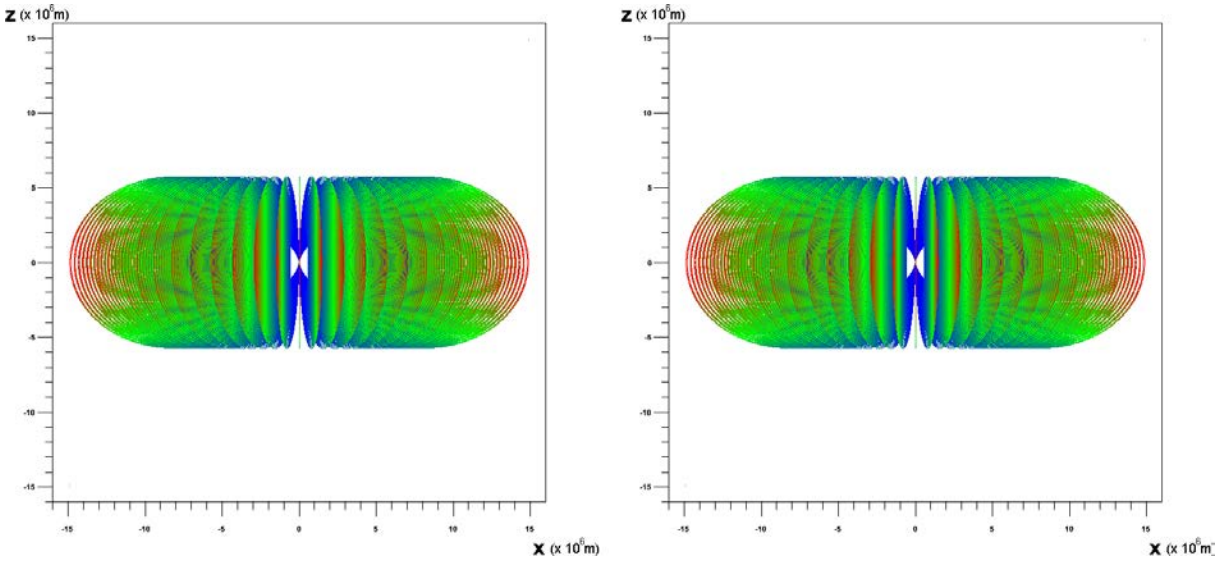

Figure 6.2: The axisymmetric case, with the magnetic dipole calculation at left and the calculation using Deutsch fields at right, for field lines that close within 1.5×10^7m.

Figure 6.3 shows the dipole field (left) and the Deutsch field in the extreme case in which the dipole moment is orthogonal to the rotation axis ($\chi = \pi/2$). Field lines closing within $0.5R_{lc}$ are plotted. The distortion in the dipolar structure of the Deutsch fields can clearly be seen for fieldlines extending along the z-axis, while the field lines near the rotational equator $z = 0$ do not extend as far radially and more or less maintain their dipolar shape. Note that the upper right panel of figure 6.3 shows the Deutsch magnetosphere to be narrower horizontally than the dipole fields; this is due to the Deutsch fields beginning to twist at large radii, as seen by comparing the bottom two panels. The viewing angle in the top right panel does not necessarily show the Deutsch magnetosphere at its maximum width, as is the case in the top left panel.

6.3 Comparison with McDonald and Shearer (2009)

McDonald and Shearer (2009) use a superposition of Deutsch fields and plasma fields in a 3D simulation to find stable charge distributions by self-consistently moving charges around until a stabilty condition is met. It is important to recognize the distinction between this type of simulation and the one carried out in this thesis: McDonald and Shearer (2009) find distributions of non-neutral plasma in which the electromagnetic forces are balanced, while our calculation finds mass distributions when the thermal, gravitational and centrifugal effects are balanced (under the assumption that the electrostatic effects of the charge separation are negligible). A full simulation including these effects in a plasma density calculation would be an ambitious, but potentially worthwhile endeavour.

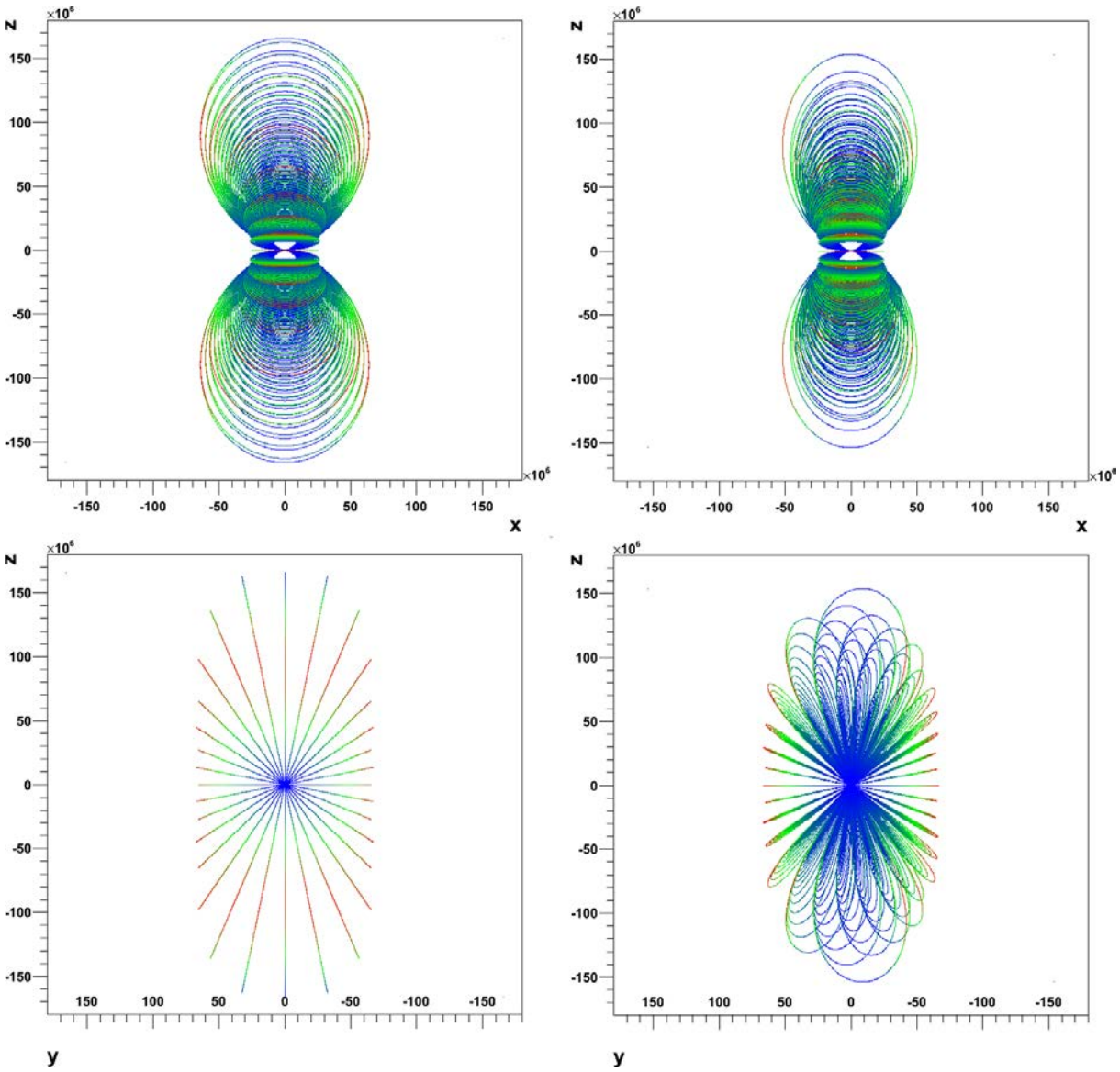

Figure 6.3: The orthogonal case, restricting field lines to one half of the light cylinder radius, $\sim 6.7\times10^7$m. The left figures shows the dipole fields and the right figures shows the Deutsch fields; the bottom figures are the same calculations rotated by 90° so that the dipole moment is out of the page. Using $\nu = 1.8$, the dipole calculation had a relative maximum and minimum density of 250 and 1×10^{-4}, while the maximum and minimum for the Deutsch field calculation were 245 and 1×10^{-3} respectively.

6.4 Comparison with Lyutikov and Thompson (2005)

Lyutikov and Thompson model the density in the magnetosphere as being concentrated uniformly on a set of field lines with maximum extension within a fairly narrow range $R_- < R_{max} < R_+$. The assumption of constant density along field lines is contrary to our approach. Further, their criterion for the maximum radius is based on estimates of the "size" of the magne-

tosphere, and so they measure this radius with respect to the magnetic equator; as a result the limiting fieldlines, and thus the density distribution, are axially symmetric about the magnetic axis. Equations 3.9 and 3.10 suggest that the density distribution should be axially symmetric about the rotation axis, at least for initial points satisfying this symmetry; however when we restrict the calculation to field lines that close within a certain radius we obtain a density distribution that is not symmetric about either axis. When our calculation is restricted to a similar maximum radius we find relative densities ranging from 1 at the initial radius $r = 100$km down a minimum of about $1{\times}10^{-4}$ (blue) before increasing to about 4.5 (red), when the parameter $\nu = 1.8$. Lower values of ν have the effect of increasing the maximum and decreasing the minimum. Given these considerations, we raise two issues with the model due to Lyutikov and Thompson (2005):

1. Their selection of which field lines to include uses a maximum distance measured along the magnetic equator, rather than along the equator of rotation. In our model we suppose that the ability of a field line to support an equilibrium plasma density depends on how closely it approaches to the light cylinder, and so the shape of the limiting field lines we include depends on the angle χ. In fitting the angle χ, Lyutikov and Thompson's magnetosphere stays the same shape.

2. Their model neglects to consider the equilibrium density along field lines, and assuming constant density seems to be a gross oversimplification.

As a possible explanation of their results, we note that the high density regions we calculate seem to lie approximately in a plane, which is not normal to the dipole moment or the axis of rotation, but is inclined somewhere between. If this was primarily the matter affecting the eclipse, then under Lyutikov and Thompson's assumptions the dipole moment is normal to this plane, which leads to an underestimation of the angle χ. One can then ask if there is angle χ, in our model, which gives a density distribution concentrated around a plane normal to Lyutikov and Thompson's best fit for the parameter χ, in the hopes that our density distribution can reproduce the eclipse light curve with a different value of χ. Figures 6.7 and 6.8 show calculations with the Deutsch fields for $\chi = 80^\circ$ and $\chi = 85^\circ$ respectively. As χ approaches 90° the distribution becomes complicated, but we attempt to draw a line (really a plane extending into the page) around which the density distribution is roughly centered.

This idea weakly suggests that the angle χ is closer to 90° than predicted by Lyutikov and Thompson (2005), though a detailed study is clearly necessary since our density curves are drastically different than theirs.

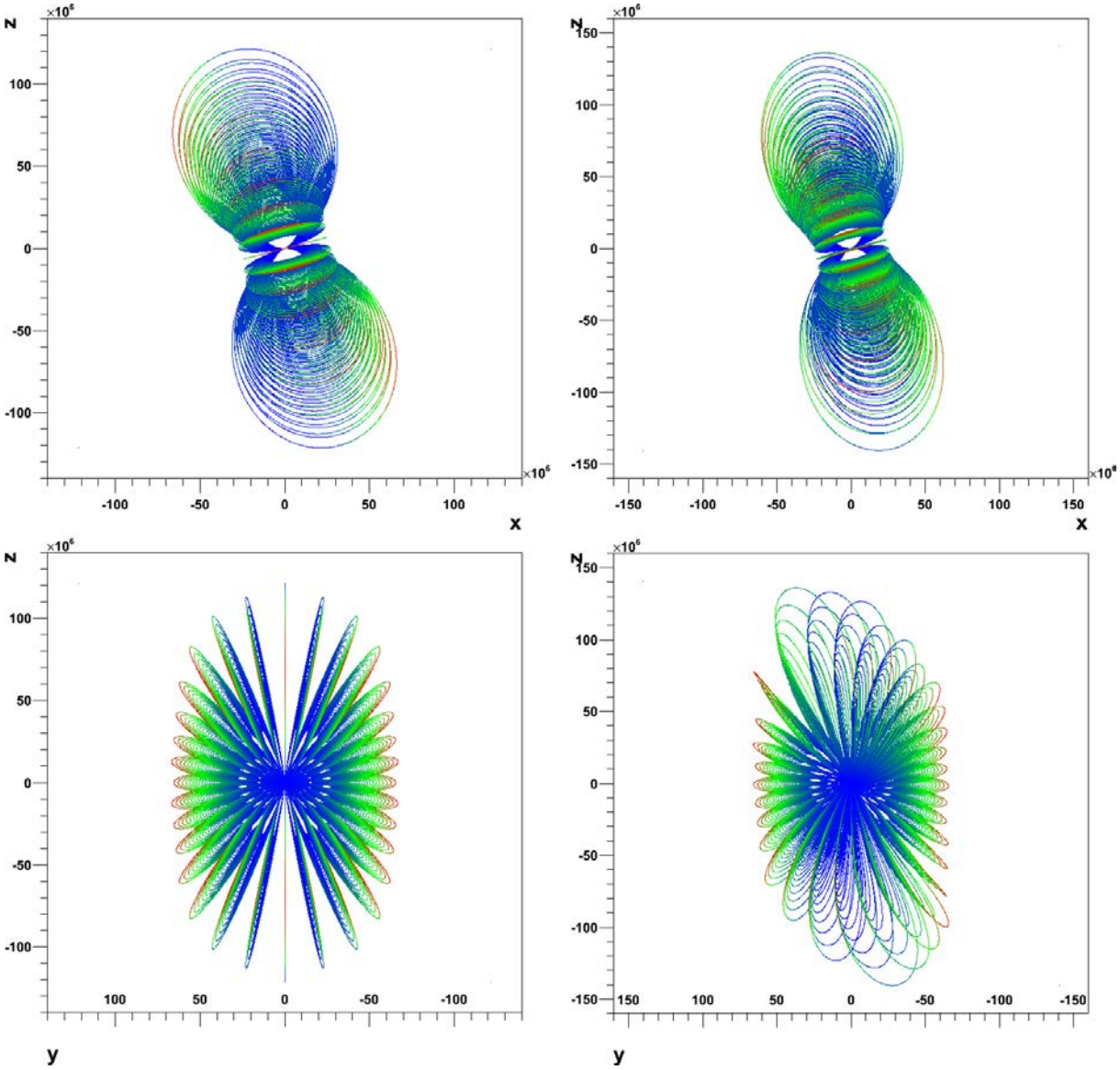

Figure 6.4: Using Lyutikov and Thompson's best fit value $\chi = 75°$, the magnetic field lines have been allowed to extend to one half the light cylinder radius at the rotational equator. The dipole fields (left) and Deutsch fields (right) show significant differences at this radius. The bottom frames show the same calculations rotated by 90°. In the dipole calculation the relative density reached a maximum of 250 and a minimum of 1.4×10^{-4}, and in the Deutsch field calculation it reached a maximum of 252 and a minimum of 7.7×10^{-4}.

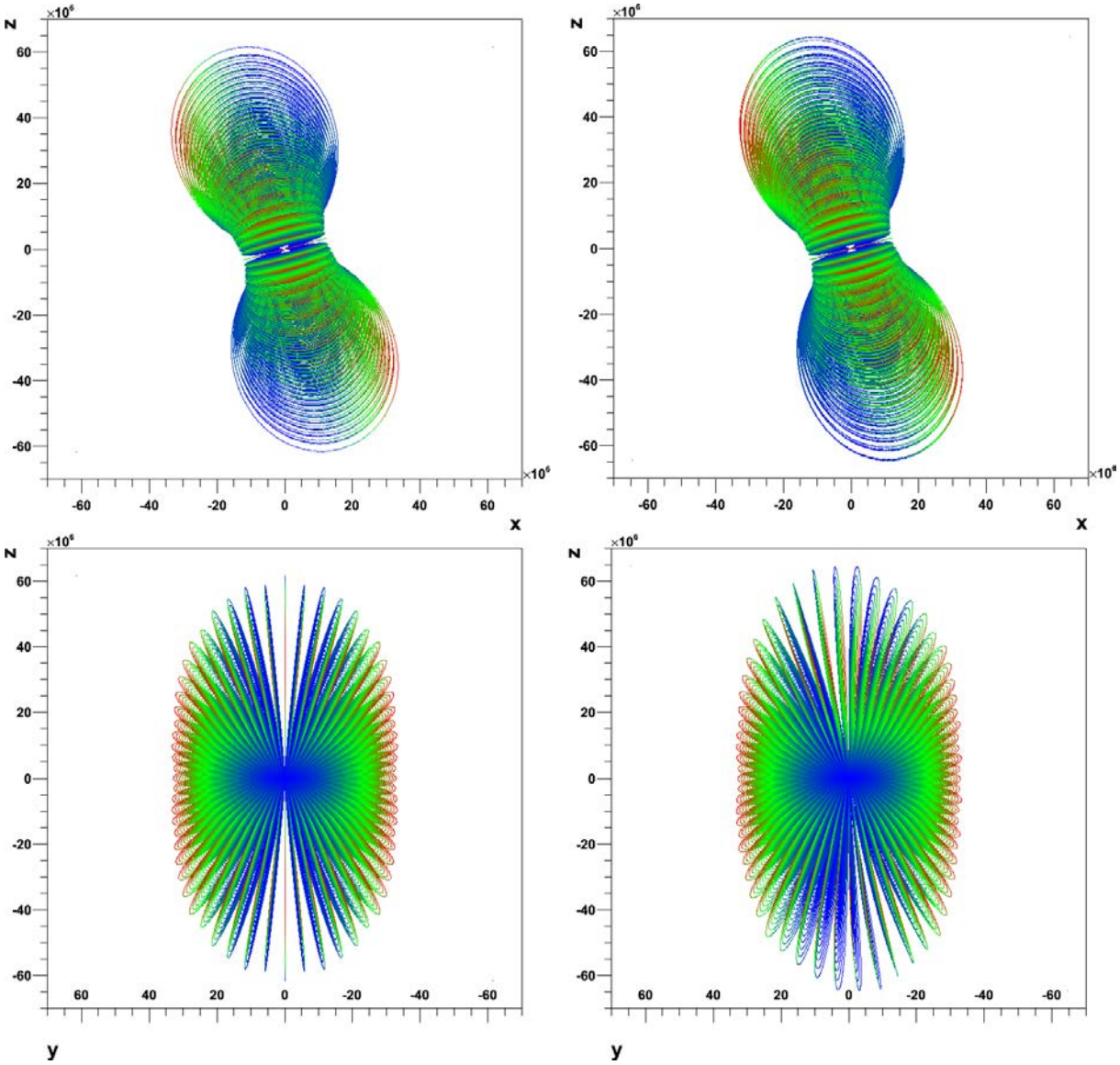

Figure 6.5: Using the same parameters as in 6.4, but restricting the field lines to those close within one quarter of the light cylinder radius, as measured at the rotational equator. Significant differences between the fields are still seen. The bottom frames show the same calculations rotated by 90°. In the dipole calculation the relative density reached a maximum of 36 and a minimum of 3.5×10^{-4}, and in the Deutsch field calculation it reached a maximum of 35.9 and a minimum of 7.7×10^{-4}.

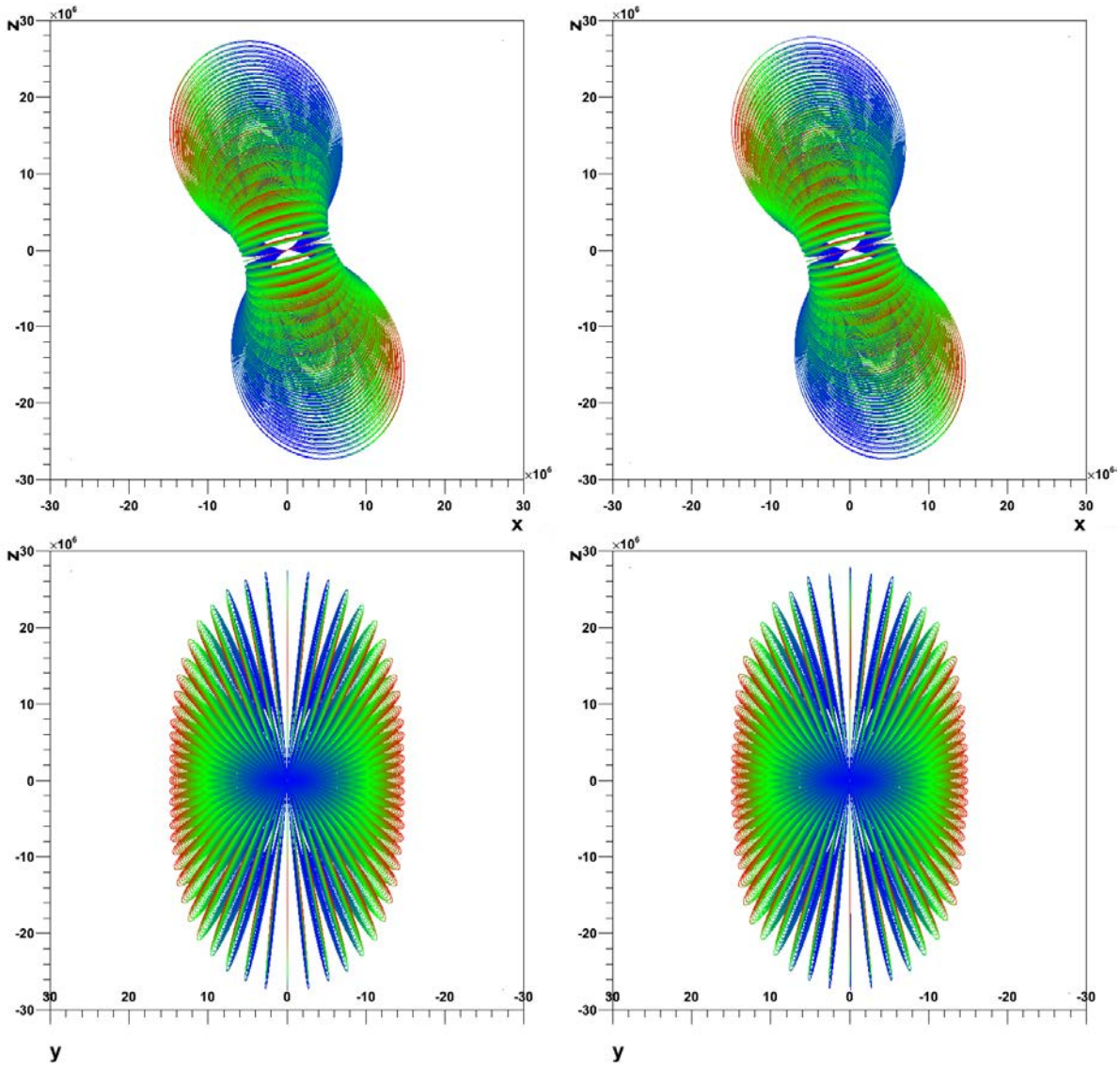

Figure 6.6: Once again using the same parameters as in 6.4, we now restrict the field lines to those close within 1.5×10^7m $\sim 0.11R_{lc}$, as measured at the rotational equator. The fields appear similar at this scale. The bottom frames show the same calculations rotated by 90°. In the dipole calculation the relative density reached a maximum of 4.61 and a minimum of 9.5×10^{-4}, and in the Deutsch field calculation it reached a maximum of 4.63 and a minimum of 9.4×10^{-4}.

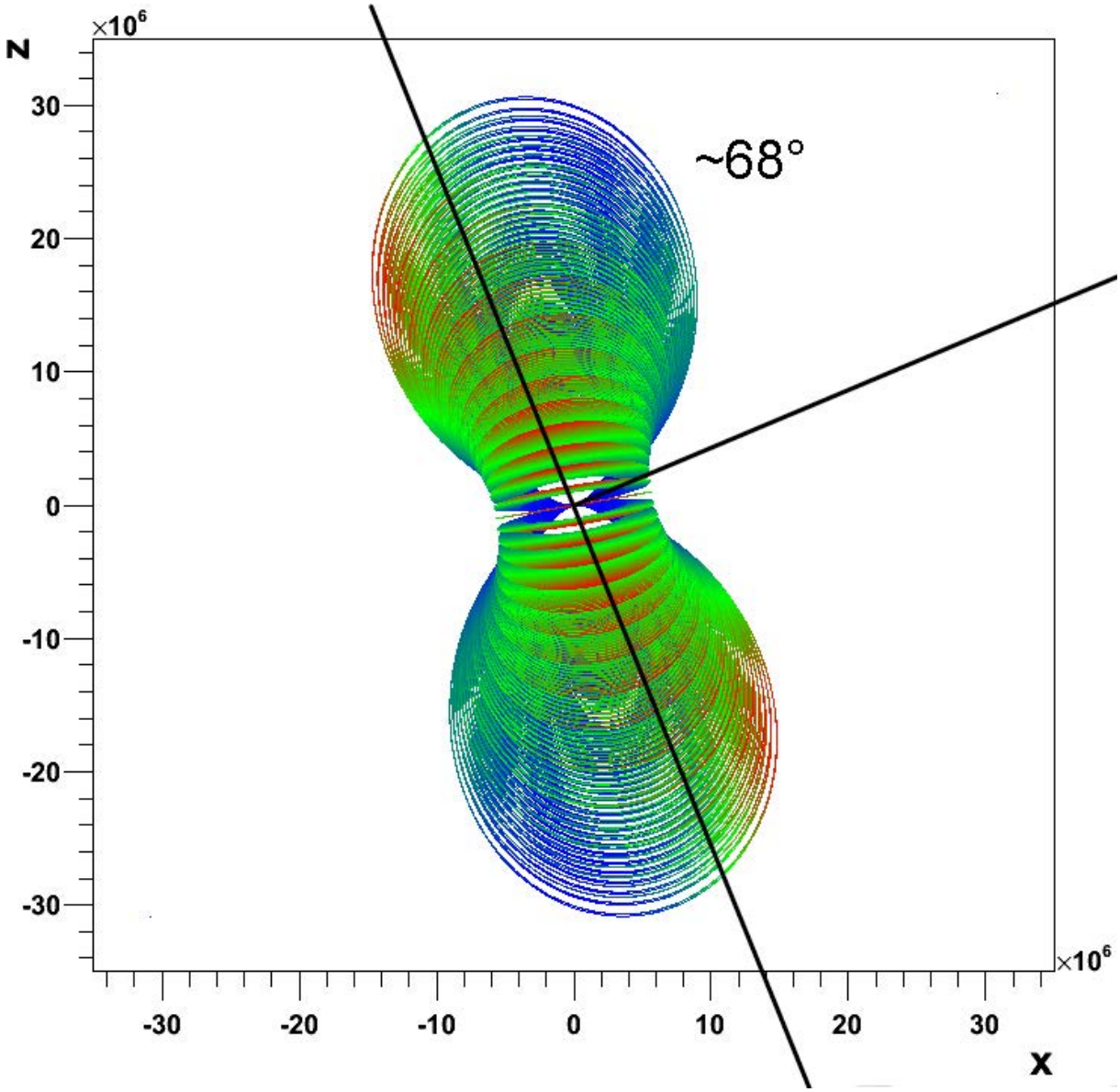

Figure 6.7: The Deutsch field lines closing within 1.5×10^7m are shown for $\chi = 80°$. A line is drawn representing a plane about which the density is roughly centered. A perpendicular line represents the normal to this plane, which Lyutikov and Thompson's analysis implicitly takes to coincide with the dipole moment. We find this line to be at an angle of about 68°, though placement of the line is very subjective.

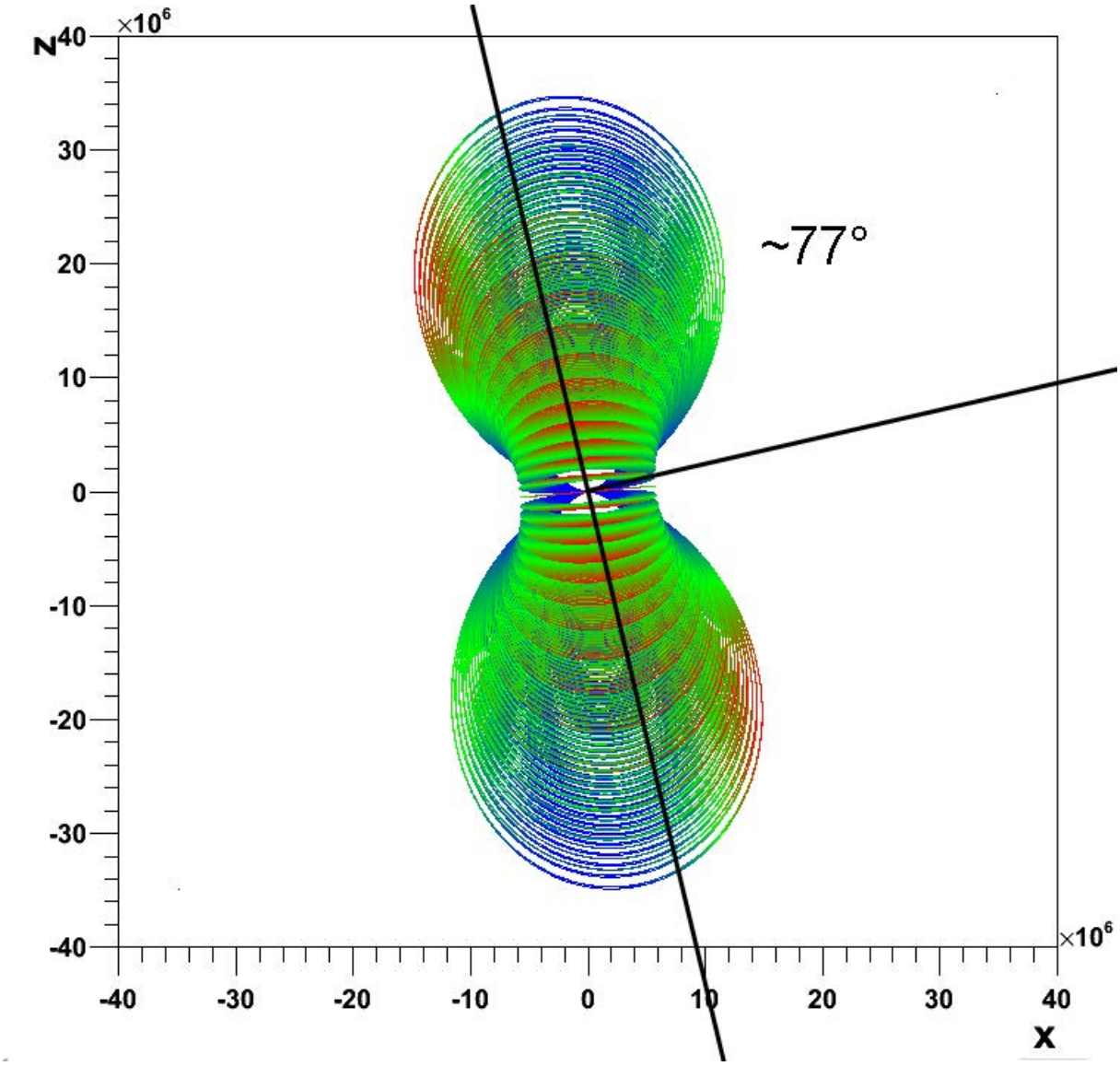

Figure 6.8: The Deutsch field lines closing within 1.5×10^7m are shown for $\chi = 85°$. A line is drawn representing a plane about which the density is roughly centered, but in this case the distribution is more complicated and the uncertainty in the slope is even larger. We give a value of about 77° for angle the normal to this plane makes with the rotation axis, though we recognize that the distribution takes on a new structure as θ approaches 90°.

7
Conclusions

Our approach is novel to that in the literature, and gives results inconsistent with the ideas of Lyutikov and Thompson (2005) in particular. The shape of the absorbing material, as well as the plasma density distribution within it, is seen to change with the angle χ. The density along field lines closing within some radius decreases away from the pulsar until the effects of corotation become significant and the density rises dramatically. It is clear that a full simulation of the eclipse light curve, along with an independent fitting of parameters, is necessary in order to fully evaluate our model in the context of the pulsar B. Our results differ drastically from Lyutikov and Thompson's, so it is not clear whether or not a best fit to our model would provide a slight modification of their parameters or a completely different set of parameters.

Within the radius $r = 1.5 \times 10^7$m which Lyutikov and Thompson associate with the edge of the magnetosphere, we have seen that the magnetic dipole is a good approximation to the Deutsch fields. However, the Deutsch fields begin to become important if the magnetosphere is much bigger than this, particularly if the angle χ is large, since the field lines are allowed to extend in the z-direction.

We have neglected electrostatic effects, which appear as an additional term in equation 3.9 proportional to the average charge separation of the plasma. In contrast to McDonald and Shearer (2009), our method says nothing about how charge density is distributed at electrostatic equilibrium. This is an added complication which merits further study.

While this work does not say very much conclusively, our results encourage further research along these lines. In particular, the integral of the motion (3.9) gives useful information that could be used in conjunction with an eclipse light curve analysis.

References

R. Breton, V. Kaspi, M. Kramer, and M. McLaughlin. Relativistic spin precession in the double pulsar. *Science*, 2008. 3

A. J. Deutsch. The electromagnetic field of an idealized star in rigid rotation in vacuo. *Annales d'Astrophysique, Vol. 18*, 1955. 9

V. Fock. Theory of space, time and gravitation. *Pergamon Press Ltd.*, 1964. 5, 7

R. Henriksen and M. Higgins. The deutsch field gamma ray pulsar. *Royal Astronomical Society*, 1997. v, 10

R. Henriksen and D. Rayburn. Hot pulsar magnetospheres. *Royal Astronomical Society*, 1973. ii, 1, 5, 7

M. Higgins. Gamma-ray emmision from neutron stars and the deutsch field pulsar. *Ph.D Thesis, Queen's University*, 1996. 10

M. Lyutikov and C. Thompson. Magnetospheric eclipses in the double pulsar system psr j0737-3039. *The Astrophysical Journal*, 2005. ii, iii, v, 1, 2, 3, 4, 9, 10, 12, 15, 16, 17, 19, 21, 23

John McDonald and Andrew Shearer. Investigations of the magnetospheric plasma distribution in the vicinity of a pulsar. *The Astrophysical Journal*, 2009. iii, 10, 14, 23

M. A. McLaughlin, A. G. Lyne, and D. R. Lorimer. The double pulsar system j0737-3039: modulation of a by b at eclipse. *The Astrophysical Journal*, 2004. v, 4

I. A. Morrison, T. W. Baumgarte, S. L. Shapiro, and V. R. Pandharipande. The moment of inertia of the binary pulsar j0737-3039a: Constraining the nuclear equation of state. *The Astrophysical Journal*, 2004. 6

A. Quadir, R. Ruffini, and G. Violini. On the rotational energy loss of pulsars. *Lettere Al Nuovo Cimento*, 1980. 10